

Trioxorhenium and Trioxotechnetium as Strong Acceptor Groups. 3. Charge Transfer and Bonding Energetics in $O_3M-M(CO)_5$ ($M = Re, Tc$)¹

Miquel Costas,[†] Josep M. Poblet,^{*,†} Marie-Madeleine Rohmer,[‡] and Marc Bénard^{*,‡}

Departament de Química, Universitat Rovira i Virgili, 43005 Tarragona, Spain, and Laboratoire de Chimie Quantique, UPR 139 du CNRS, Université Louis Pasteur, F-67000 France

Received March 3, 1994[⊗]

Ab initio SCF, two-configuration (TC) SCF, and CI calculations have been carried out to investigate the bonding potentialities of Re(VI) in trioxorhenium with Re(0) in $Re(CO)_5$. Calculations show that the electron-withdrawing character of ReO_3 makes the hypothetical $O_3Re-Re(CO)_5$ binuclear complex a highly polar molecule. The charge transfer toward trioxorhenium (0.534 e) is not so large, however, as in $O_3Re-ReCl_2(dmpm)_2$, the only bimetallic complex characterized to date with ReO_3 . In both $O_3Re-Re(CO)_5$ and $O_3Re-ReCl_2(dmpm)_2$, the metal–metal coupling can be expressed in terms of a σ donation from the most oxidized rhenium atom to the least oxidized one. The topological analysis of the Laplacian distribution of density shows that the bonding of the ReO_3 fragment is mostly ionic. The critical points of the Laplacian distribution characterized along the metal–metal bond axis are typical of a σ donation, but also evidence some covalent character. The energy associated with a homolytic dissociation is computed to be 271 kJ mol⁻¹, accounting for the geometrical relaxation of the ligands. This value is larger than the Re–L bond energies previously computed for various types of O_3Re-L molecules. An investigation carried out on $O_3Tc-Tc(CO)_5$ leads to similar results.

1. Introduction

One of the most active trends in organometallic chemistry and catalysis is the search for new routes to couple within the same molecule various metal sites displaying different chemical activities.² Concerning homobinuclear complexes, dissymmetry should be sought from different coordination spheres around each center, possibly leading to distinct oxidation states for the two metals.^{3–6} Such cases of intramolecular disproportionation were evidenced first for molecules displaying multiple metal–metal bonds,⁴ but this class of asymmetric complexes was

recently enlarged by the characterization of various molecules exhibiting not so tight metal–metal coupling.^{5,6} Interesting potentialities, not fully explored yet, seem to be offered in this area by trioxorhenium ReO_3 and related trioxides. On the one hand, Ara, Fanwick, and Walton (AFW) have characterized $O_3-ReReCl_2(dmpm)_2$, a dirhenium(VI,II) complex with a strong metal–metal single bond,⁶ and, quite recently, the structure of a $Pt_3(ReO_3)$ cluster cation was reported by Xiao et al.⁷ On the other hand, Beattie and Jones⁸ and then Herrmann and co-workers⁹ have shown that ReO_3 is susceptible to give covalent bonds with CH_3 and various aryl ligands. Mealli et al. have recently provided a qualitative MO interpretation of the metal–carbon bond homolysis in those complexes.¹⁰ X- ReO_3 complexes are also known with halogens.¹¹ An obvious application of the isolobal analogy¹² suggests that a similar coupling could be expected with 17-electron moieties such as $Re(CO)_5$, thus giving rise to a novel class of homobinuclear complexes displaying intramolecular disproportionation. The goal of the present paper is to investigate the nature and the strength of the metal–metal bond in the hypothetical complexes $O_3M-M(CO)_5$ ($M = Re, Tc$) and to discuss the feasibility of such molecules by comparison with previous ab initio MO studies

[†] Universitat Rovira i Virgili.

[‡] Université Louis Pasteur.

[⊗] Abstract published in *Advance ACS Abstracts*, November 15, 1994.

- (1) Previous papers in the series: (a) Costas, M.; Leininger, T.; Jeung, G.-H.; Bénard, M. *Inorg. Chem.* **1992**, *31*, 3317–3321. (b) Wiest, R.; Leininger, T.; Jeung, G.-H.; Bénard, M. *J. Phys. Chem.* **1992**, *96*, 10800–10804.
- (2) For recent reviews, see ref 1 in our ref 1a.
- (3) Walton, R. A. In *Metal-Metal Bonds and Clusters in Chemistry and Catalysis*; Fackler, J. P., Ed.; Plenum: New-York, 1990; pp 7–17.
- (4) (a) Chakravarty, A. R.; Cotton, F. A.; Cutler, A. R.; Tetric, S. M.; Walton, R. A. *J. Am. Chem. Soc.* **1985**, *107*, 4795–4796. (b) Chakravarty, A. R.; Cotton, F. A.; Cutler, A. R.; Walton, R. A. *Inorg. Chem.* **1986**, *25*, 3619–3624. (c) Bennett, M. J.; Cotton, F. A.; Walton, R. A. *J. Am. Chem. Soc.* **1968**, *88*, 3866–3867. (d) Bennett, M. J.; Cotton, F. A.; Walton, R. A. *Proc. R. Soc. London A* **1968**, *303*, 175–192. (e) Anderson, R. A.; Jones, R. A.; Wilkinson, G. J. *Chem. Soc., Dalton Trans.* **1978**, 446–453. (f) Chisholm, M. H.; Huffman, J. C.; Van Der Sluys, W. G. *J. Am. Chem. Soc.* **1987**, *109*, 2514–2515.
- (5) (a) Bonrath, W.; Michaelis, M.; Pörschke, K. R.; Gabor, B.; Mynott, R.; Krüger, C. *J. Organomet. Chem.* **1990**, *397*, 255–260. (b) Michaelis, M.; Pörschke, K. R.; Mynott, R.; Goddard, R.; Krüger, C. *Ibid.* **1992**, *426*, 131–141. (c) Chisholm, M. H.; Cook, C. M.; Foltz, K. *J. Am. Chem. Soc.* **1992**, *114*, 2721–2722. (d) Alt, H. G.; Hayen, H. I.; Rogers, R. D. *J. Chem. Soc., Chem. Commun.* **1987**, 1795–1796. (e) Schäfer, R.; Kaim, W.; Fiedler, J. *Inorg. Chem.* **1993**, *32*, 3199–3200. (f) Chisholm, M. H.; Cook, C. M.; Huffman, J. C.; Martin, J. D. *Organometallics* **1993**, *12*, 2354–2359. (g) Sinnema, P.-J.; Meetsma, A.; Teuben, J. H. *Ibid.* **1993**, *12*, 184–189. (h) Bartley, S. L.; Dunbar, K. R.; Shih, K.-Y.; Fanwick, P. E.; Walton, R. A. *Inorg. Chem.* **1993**, *32*, 1341–1349.
- (6) (a) Ara, I.; Fanwick, P. E.; Walton, R. A. *J. Am. Chem. Soc.* **1991**, *113*, 1429–1431. (b) Ara, I.; Fanwick, P. E.; Walton, R. A. *Inorg. Chem.* **1993**, *32*, 2958–2962.

(7) Bailey, M. F.; Dahl, L. F. *Inorg. Chem.* **1965**, *4*, 1140–1145.

(8) Beattie, I. R.; Jones, P. J. *Inorg. Chem.* **1979**, *18*, 2318–2319.

(9) (a) Herrmann, W. A.; Ladwig, M.; Kiprof, P.; Riede, J. *J. Organomet. Chem.* **1989**, *371*, C13–C17. (b) Herrmann, W. A.; Romão, C. C.; Fischer, R. W.; Kiprof, P.; de Méric de Bellefon, C. *Angew. Chem. Int. Ed. Engl.* **1991**, *30*, 185–187. (c) Herrmann, W. A.; Kiprof, P.; Rypdal, K.; Tremmel, J.; Blom, R.; Alberto, R.; Behm, J.; Albach, R. W.; Bock, H.; Solouki, B.; Mink, J.; Lichtenberger, D.; Gruhn, N. E. *J. Am. Chem. Soc.* **1991**, *113*, 6527–6537. (d) de Méric de Bellefon, C.; Herrmann, W. A.; Kiprof, P.; Whitaker, C. *Organometallics* **1992**, *11*, 1072–1081.

(10) Mealli, C.; López, J. A.; Calhorda, M. J.; Romão, C. C.; Herrmann, W. A. *Inorg. Chem.* **1994**, *33*, 1139–1143.

(11) (a) Lotspeich, J. F.; Javan, A.; Engelbrecht, A. *J. Chem. Phys.* **1959**, *31*, 633–643. (b) Lotspeich, J. F. *Ibid.* **1959**, *31*, 643–649.

(12) (a) Hoffmann, R. *Angew. Chem., Int. Ed. Engl.*, **1982**, *21*, 711–724. (b) Albright, T. A.; Burdett, J. K.; Whangbo, M. H. *Orbital Interactions in Chemistry*, Wiley: New-York, 1985; pp 352–356.

carried out on the dinuclear complex O₃ReReCl₂(H₂PCH₂PH₂)₂^{1a} and on monometallic O₃R–L molecules (L = CH₃, CF₃, Cl, F).^{1b,13}

2. Computational Details

2.1 Basis Sets. Ab initio SCF, two-configuration (TC)-SCF,¹⁴ and CI calculations on O₃ReRe(CO)₅ have been carried out by means of the ASTERIX program system,¹⁵ modified for core potential evaluation.¹⁶ We employed the relativistic core potential of Christiansen et al.¹⁷ for the Re atoms, leaving the 5s and 5p shells out of core. The 15 remaining electrons are described with an optimized 6s,5p,5d basis set contracted into 4s,4p,4d and including diffuse functions. For the carbon monoxide ligands, all electron basis sets were adapted from the 9s5p sets optimized by Huzinaga.¹⁸ Diffuse exponents were added to the s shell for carbon ($\zeta_s = 0.05$) and to the s and p shells for oxygen ($\zeta_s = 0.05$, $\zeta_p = 0.07$), and both sets were contracted to 4s,3p, which is minimal for the 1s shell and triple- ζ for the valence shell. The same split-valence basis set was employed for the oxygen atoms of trioxorhenium during the geometry optimization process. However, the TCSCF and CI calculations on the optimal geometry have been carried out with an improved basis set for the formally O²⁻ oxygens of trioxorhenium. This 11s,7p basis set was taken from Huzinaga,¹⁹ it includes one s and one p diffuse function ($\zeta_s = 0.0752$, $\zeta_p = 0.0515$), and it is contracted to 6s,4p according to Dunning's procedure.²⁰

For O₃TcTc(CO)₅, the all-electron basis set optimized by Hyla-Kryspin et al. for technetium²¹ was incremented with one diffuse d function ($\zeta_d = 0.075$), leading to a 14s,9p,8d basis set contracted to 6s,4p,4d. For C and O atoms, Huzinaga's split-valence basis sets of size 9s,5p¹⁸ without diffuse functions and contracted into 3s,2p were used for the gradient optimization process carried out with the TURBOMOLE program.²²

The final TCSCF and CI calculations were carried out with ASTERIX using the more extended split-valence basis sets of contracted size 4s,3p already employed for the geometry optimization of the rhenium complex. The 6s,4p basis set specifically used for the oxygen atoms of ReO₃ has not been employed for the calculations on the technetium complex.

2.2 Calculation of the Bond Energies. The procedure used to compute the bond energy between the two metal fragments is similar to the strategy designed to estimate the Re–L bond energy in O₃Re–L complexes.^{1b} TCSCF calculations were carried out on the bimetallic complexes O₃MM(CO)₅ (M = Re, Tc), the reference space being composed of the $\sigma^2\sigma^*$ and $\sigma^0\sigma^*$

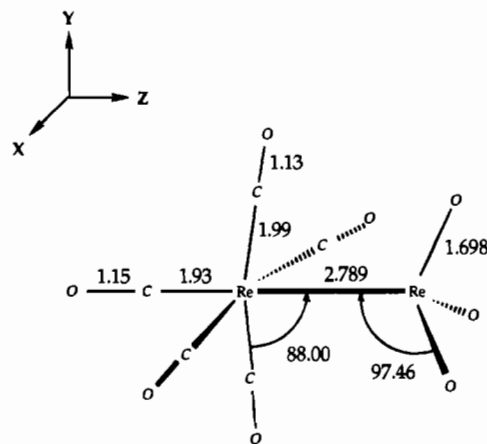


Figure 1. O₃Re–Re(CO)₅: geometry optimized (for part) at the SCF level of calculation. The Re–C and C–O distances were taken from ref 24.

configurations. The correlation of the metal–metal coupling was then completed by a two-reference CI expansion accounting for all possible excitations of the two σ electrons. A similar procedure has been used for the calculation of the negatively charged fragments. Neutral and cationic fragments have been computed at the SCF level. For ReO₃–Re(CO)₅, the dissociation energy was then computed at a more extended level of CI. Twenty-six electrons were correlated, formally belonging to the metal–metal σ and σ^* orbitals (reference space, 2 electrons), to the metal d shell of Re(CO)₅ (6 electrons), and to the outer valence shell of ReO₃ (18 electrons). The same set of 26 electrons was correlated in a supersystem composed of the Re(CO)₅ and ReO₃ radical fragments in their respective optimal geometries, with $d_{\text{Re–Re}}$ sufficiently large to make all interactions vanish. The CI expansions were carried out using Siegbahn's contracted CI program.²³

3. Results and Discussion

3.1 Geometry Optimization. The geometry optimization of the complex O₃ReRe(CO)₅ has been subject to the following constraints: (i) local symmetries C_{3v} for ReO₃ and C_{4v} for Re(CO)₅ have been maintained in the dinuclear complex and (ii) the Re–C and C–O distances were not optimized but transposed from the parameters observed in the homobinuclear complex Re₂(CO)₁₀.²⁴ To be consistent, this constraint was also applied to the isolated fragments Re(CO)₅ and [Re(CO)₅]⁺ for which the only parameter to be optimized was the pyramidalization angle. At last, (iii) a C_s symmetry was imposed to the complex assuming one Re–CO and one Re–O bond to be coplanar. This is not a real constraint, since a rotation by 15° of the ReO₃ moiety with respect to Re(CO)₅ leads to an energy identical within 0.05 kJ mol⁻¹ to that of the molecule with C_s symmetry. The geometry optimized at the closed-shell SCF level assuming those conditions is displayed in Figure 1. The Re–Re distance was found to be 2.789 Å, shorter by 0.26 Å than the metal–metal distance in dirhenium decacarbonyl (3.041 Å), but longer by 0.32 Å than the Re–Re bond length in O₃Re–ReCl₂(dmpm)₂. One should be reminded that the Re–Re coupling in all three complexes is formally described in terms of a single metal–metal bond. It is clear that this remarkably large range of bond distances implies important differences concerning the real bonding modes.

(13) Szyperki, T.; Schwerdtfeger, P. *Angew. Chem. Int. Ed. Engl.* **1989**, *28*, 1228–1231.

(14) Wood, M. H.; Veillard, A. *Mol. Phys.* **1973**, *26*, 595–603.

(15) (a) Ermenwein, R.; Rohmer, M.-M.; Bénard, M. *Comput. Phys. Commun.* **1990**, *58*, 305–328. (b) Rohmer, M.-M.; Demuyneck, J.; Bénard, M.; Wiest, R.; Bachmann, C.; Henriet, C.; Ermenwein, R. *Ibid.* **1990**, *60*, 127–144. (c) Wiest, R.; Demuyneck, J.; Bénard, M.; Rohmer, M.-M.; Ermenwein, R. *Ibid.*, **1991**, *62*, 107–124. (d) Rohmer, M.-M.; Ermenwein, R.; Ulmschneider, M.; Wiest, R. *Int. J. Quantum Chem.* **1991**, *40*, 723–743.

(16) Leininger, T.; Jeung, G.-H., unpublished work.

(17) Ross, R. B.; Powers, J. M.; Atashroo, T.; Ermler, W. C.; LaJohn, L. A.; Christiansen, P. A. *J. Chem. Phys.* **1990**, *93*, 6654–6670.

(18) (a) Huzinaga, S. *Approximate Atomic Functions*, Technical Report, University of Alberta, Canada, 1971. (b) Huzinaga, S.; McWilliams, D.; Domsy, B. *J. Chem. Phys.* **1971**, *54*, 2283–2284.

(19) Huzinaga, S. *J. Chem. Phys.* **1965**, *42*, 1293–1302.

(20) Dunning, T. H. *J. Chem. Phys.* **1971**, *55*, 716–723.

(21) Hyla-Kryspin, I.; Demuyneck, J.; Strich, A.; Bénard, M. *J. Chem. Phys.* **1981**, *75*, 3954–3961.

(22) TURBOMOLE: a direct SCF program from the Quantum Chemistry Group of the University at Karlsruhe under the directorship of Prof. R. Ahlrichs; Ahlrichs, R.; Bär, M.; Häser, M.; Horn, H.; Kölmel, C. *Chem. Phys. Lett.* **1989**, *162*, 165–169.

(23) Siegbahn, P. E. M. *Int. J. Quantum Chem.* **1983**, *23*, 1869–1889. The CI program has been interfaced with ASTERIX by C. Daniel, M.-M. Rohmer, and M. Spéri.

(24) Churchill, M. R.; Amoh, K. N.; Wasserman, H. J. *Inorg. Chem.* **1981**, *20*, 1609–1611.

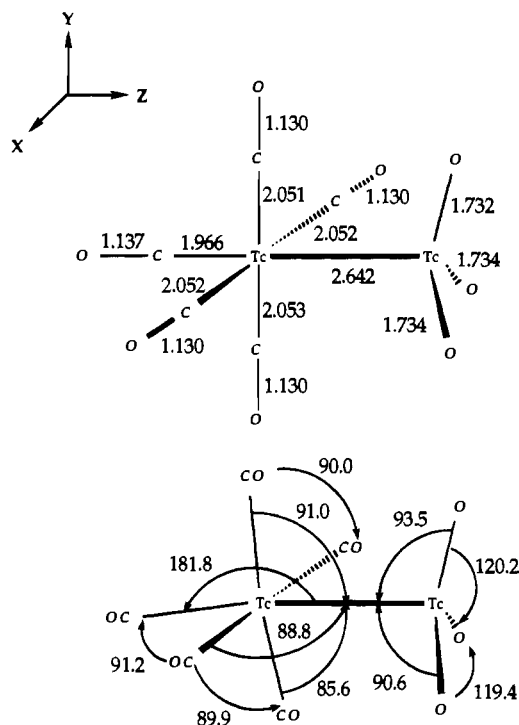


Figure 2. $\text{O}_3\text{Tc}-\text{Tc}(\text{CO})_5$: fully optimized geometry (SCF level of calculation).

The other geometrical parameters are more easily rationalized. The starting value of 1.71 Å, selected for the Re–O distance in agreement with various experimental determinations,⁹ was hardly modified to 1.698 Å (Figure 1). The same distance (1.699 Å) had been previously optimized for the isolated, neutral, and planar ReO_3 .¹ The $[\text{ReO}_3]^-$ anion, also planar, has a Re–O distance of 1.726 Å. X-ray diffraction studies carried out on various mononuclear complexes of trioxorhenium have shown that ReO_3 reacts to the presence of polyatomic ligands like CH_3 , C_5H_5 , or C_5Me_5 by a pyramidalization of the trioxorhenium moiety that may reach 114.4° for $\text{O}_3\text{Re}-\text{CpMe}$.²⁵ This pyramidalization is however energetically unfavorable,¹ and the longer Re–L distances characteristic of dirhenium complexes logically reduce the steric strain and the subsequent pyramidalization. The observed Re–Re–O angles range from 97.2° to 98° in $\text{O}_3\text{ReReCl}_2(\text{dmpm})_2$,⁶ and the value optimized in the present complex is quite comparable (97.5°). As in $\text{Re}_2(\text{CO})_{10}$, the equatorial carbonyls are very slightly bent toward the other fragment (Re–Re–C = 88°). This angle is 84.6° in the neutral, isolated fragment $\text{Re}(\text{CO})_5$ and 89° in $[\text{Re}(\text{CO})_5]^+$.

The equivalent complex of technetium, $\text{O}_3\text{TcTc}(\text{CO})_5$, has been subjected to a complete geometry optimization, assuming as for the rhenium complex a C_s symmetry. The calculated geometry is displayed in Figure 2. The optimized metal–carbon bond lengths, axial as equatorial, are longer by 0.03–0.07 Å than those observed in $\text{Tc}_2(\text{CO})_{10}$.²⁶ This should be attributed to the well-documented trend of SCF optimization to overestimate the M–CO bond lengths because of a poor description of the π back-bonding. It should be noted however that the Tc–O bond length obtained for the TcO_3 moiety (1.73 Å) is also longer than the optimized Re–O distance by the same order of magnitude. The pyramidalization of both fragments appears negligible (Figure 2). Finally, the Tc–Tc distance was found to be 2.642 Å. The isolated fragments TcO_3 , $[\text{TcO}_3]^-$, $\text{Tc}(\text{CO})_5$,

Table 1. Electron Affinity (EA, eV) and Ionization Potential (IP, eV) of Trioxorhenium Compared to Those of the Chlorine Atom and Computed Energies (hartrees) of ReO_3 ,^a Cl ,^b and Their Ions at the Ab Initio Restricted Hartree–Fock (RHF) and Configuration Interaction (CI) Levels^c

	ReO_3		Cl	
	RHF	CI	RHF	CI
cation	–302.272 928	–302.784 627	–459.022 389	–459.048 501
neutral	–302.704 483	–303.207 059	–459.456 158	–459.496 058
anion	–302.836 085	–303.330 638	–459.551 411	–459.610 401
EA	3.58	3.36	2.59	3.11
IP	11.74	11.49	11.80	12.18
electro-negativity ^d	7.66	7.42	7.19	7.65

^a Calculations on the trioxorhenium fragment have been carried out using the optimal geometries respectively determined for the neutral radical, the cation, and the anion. ^b The 12s9p basis set of Huzinaga¹⁸ was augmented with one s and one p diffuse functions and contracted to 7s6p. ^c All valence electrons have been correlated through a single reference SDCI expansion. ^d According to Mulliken's definition based upon an averaging of IP and EA values.

Table 2. Mulliken Charge of the MO_3 Fragment (q , electrons) and M–L Bond Energy (D_e , kJ mol^{-1}) Computed for Some $\text{O}_3\text{M}-\text{L}$ Complexes

	q	D_e^a	D_e^b	ref
$\text{O}_3\text{Re}-\text{F}$	0.28	324	267	1b
$\text{O}_3\text{Re}-\text{Cl}$	–0.14	236	179	1b
$\text{O}_3\text{Re}-\text{C}_5\text{H}_5$	–0.44	208	102	1b
$\text{O}_3\text{Re}-\text{CH}_3$	–0.14	319	237	1b
$\text{O}_3\text{Re}-\text{CF}_3$	–0.06	211	177	1b
$\text{O}_3\text{Re}-\text{ReCl}_2(\text{H}_2\text{PCH}_2\text{PH}_2)_2$	–0.79	500	78	1a
$\text{O}_3\text{Re}-\text{Re}(\text{CO})_5$	–0.53	285	271	this work
$\text{O}_3\text{Tc}-\text{Tc}(\text{CO})_5$	–0.71	321	299	this work

^a Dissociation energy with respect to unrelaxed fragments. ^b Dissociation energy with respect to optimized fragments.

and $[\text{Tc}(\text{CO})_5]^+$ were separately optimized. For the neutral fragments, the optimized geometrical parameters are as follows: TcO_3 is planar, with $\text{Tc}-\text{O} = 1.713$ Å; $\text{Tc}(\text{CO})_5$ is a square pyramid with $\text{Tc}-\text{C}_{\text{ax}} = 1.938$ Å, $\text{Tc}-\text{C}_{\text{eq}} = 2.028$ Å, $\text{C}-\text{O}_{\text{ax}} = 1.141$ Å, and $\text{C}-\text{O}_{\text{eq}} = 1.143$ Å. The pyramidalization angle $\text{C}_{\text{ax}}-\text{Tc}-\text{C}_{\text{eq}}$ is 94.3° . In the ionic fragments, the metal–ligand bond lengths are larger by 0.045–0.068 Å and the $\text{C}_{\text{ax}}-\text{Tc}-\text{C}_{\text{eq}}$ angle becomes 91.3° .

Those geometrical parameters suggest that the bonding in $\text{O}_3\text{Tc}-\text{Tc}(\text{CO})_5$ is not basically different from that of the dirhenium complex, a hypothesis which is confirmed by the similarity of the charge distribution and of the bonding energetics. We will therefore concentrate the discussion on $\text{O}_3\text{Re}-\text{Re}(\text{CO})_5$ and implicitly extend the conclusions to the technetium dimer.

3.2. Electronic Structure and Charge Transfer. The key point to be kept in mind when analyzing the electronic structure of trioxorhenium products is the remarkable electron-withdrawing capacity of ReO_3 , assumed to be stronger than that of sulfonic acids.^{9c} The ionization potential and the electron affinity computed for ReO_3 at the ab initio CI level are 11.5 and 3.4 eV, respectively (Table 1). Similar calculations carried out on the chlorine atom led to 12.2 and 3.1 eV (Table 1). Mulliken's definition of electronegativity based upon an averaging of IE and EA values therefore leads to similar values for chlorine (7.65 eV) and for trioxorhenium considered as a single atom (7.42 eV). Bonding between ReO_3 and a variety of ligands such as C_5H_5 , CH_3 , CF_3 , Cl , and F is basically covalent and leads to a dissociation into neutral species. The Mulliken charge on ReO_3 is slightly negative for all such systems, except for $\text{L} = \text{F}$ (Table 2), and the computed dipole moments are oriented accordingly.^{1b}

(25) Herrmann, W. A.; Taillefer, M.; de Méric de Bellefont, C.; Behm, J. *Inorg. Chem.* **1991**, *30*, 3247–3248.

(26) Xiao, J.; Puddephatt, R. J.; Manojlovic-Muir, L.; Muir, K. W.; Torabi, A. A. *J. Am. Chem. Soc.* **1994**, *116*, 1129–1130.

In the complex characterized by Ara et al. (AFW complex), ReO₃ produces a very short Re–Re bond (2.4705 Å) with ReCl₂(dmpm)₂, in which one chlorine atom and the two chelating phosphines form the basis of a pentagonal pyramid.⁶ This crowded conformation constrains the unpaired metal electron to occupy a relatively destabilized d_{z²} orbital. This electron is therefore easily transferred to the low-lying, ligand-centered, semioccupied orbital of ReO₃, resulting in a strongly polarized complex with a charge separation of ±0.785 e. This charge transfer provides a huge stabilization energy estimated from TCSCF + CI calculations to be 500 kJ mol⁻¹. This attractive potential eventually overcomes the energy requested to activate the ReCl₂(dmpm)₂ fragment from an octahedral structure to a conformation of pentagonal pyramid penalized from the triple aspect of electronic, electrostatic, and steric interactions.^{1a} The [Pt₃(ReO₃)(μ-dppm)₃]⁺ cation characterized by Xiao et al.⁷ has not been studied yet in such detail, but the orbital diagram proposed by the authors suggests an important polarization of the cluster, the positive charge being transferred to and delocalized on the Pt₃(dppm)₃ moiety. This interpretation is in agreement with the [ReO₄]⁻ counterion being localized opposite to the ReO₃ fragment with respect to the Pt₃ plane.

The charge distribution in O₃Re–Re(CO)₅ (**1**) appears to be intermediate between the case of the mononuclear O₃Re–L molecules (weakly polar) and that of the AFW complex stabilized by the transfer of one electron to the ReO₃ moiety. As for ReCl₂(dmpm)₂, the Re(CO)₅ fragment has an unpaired electron accommodated on a semioccupied orbital with major metal character. This metal orbital, a hybrid of d_{z²} and 6s, is directed toward the incoming ReO₃ fragment. At variance from ReCl₂(dmpm)₂, however, the axial ligand, CO, is a weak donor, with little capability of pushing the semioccupied orbital (SOMO) to high energies. Furthermore, the SOMO is stabilized and delocalized due to some π interaction with the π* orbitals of the equatorial CO ligands. As a consequence, an important charge transfer toward ReO₃ still exists in O₃Re–Re(CO)₅, but it is less massive than in the AFW complex. The Mulliken population analysis leads to a charge separation of ±0.534 e between the two fragments (±0.709 e for O₃Tc–Tc(CO)₅), the MO₃ moiety obviously bearing the negative charge. Bader's topological charges obtained from an integration of the electron density into the domains defined by the surfaces of zero gradient flux²⁷ lead to similar fragment charges, ±0.556 e, in spite of a quite different distribution of charges among individual atoms. The detail of the Mulliken orbital populations displayed in Table 3 shows that the population transfer with respect to the neutral fragments is basically limited to the d_{z²}/6s hybrids of both fragments. The comparison of the d_{z²} populations in ReO₃ and Re(CO)₅, already in favor of trioxorhenium in the neutral, isolated fragments (1.01 e vs 0.63 e, due to the delocalization of the SOMO in Re(CO)₅), becomes quite unbalanced in complex **1** (1.22 e vs 0.50 e). The balance and the amount of the 6s and 6p populations are less reliable, because of the diffuse character of those orbitals, which makes controversial and somewhat arbitrary the assignment of the corresponding density either to the metal or to the ligands. On the one hand, the "topological charge" integrated for Re(VI) in **1** according to Bader's criterion (2.30 e) suggests that most of the diffuse density should be attributed to the surrounding oxygens, which are assigned a topological charge of -0.95 e. On the other hand, a plot of the electron density involved in the Re–Re σ bond, from the TCSCF calculations (Figure 3), shows that the

Table 3. Metal Net Charges and Orbital Distribution of the Population of Both Metal Atoms in O₃Re–Re(CO)₅ and in the Isolated, Unrelaxed either Ionic or Neutral^a Fragments

	O ₃ Re–Re(CO) ₅		ionic fragm		neutral fragm	
	Re(VI)	Re(0)	Re(V)	Re(I)	Re(VI)	Re(0)
	Metal Net Charge (e)					
Mulliken	0.735	0.309	0.773	0.007	1.125	-0.207
Bader ^b	2.299					
	Population of the Metal Valence Orbitals					
6s	1.494 (1.584) ^a	0.801	1.568 (1.460)	1.155	1.147 (1.053)	1.317
Σ6p	0.419 (0.530)	0.147	0.270 (0.455)	0.090	0.363 (0.518)	0.227
d _{x²-y²}	0.831 (0.796)	0.390	0.763 (0.718)	0.414	0.820 (0.775)	0.388
d _{xy}	0.811 (0.783)	1.602	0.763 (0.718)	1.605	0.820 (0.776)	1.568
d _{xz}	0.748 (0.697)	1.621	0.642 (0.643)	1.659	0.858 (0.833)	1.539
d _{yz}	0.744 (0.760)	1.624	0.642 (0.639)	1.659	0.858 (0.828)	1.539
d _{z²}	1.219 (1.133)	0.499	1.580 (1.560)	0.413	1.008 (1.067)	0.629

^a Values in parentheses refer to the orbital populations obtained for Re(VI) in O₃Re–ReCl₂(H₂PCH₂PH₂)₂.^{1a} The differences obtained for the orbital populations in the isolated ReO₃ fragments should be attributed to the more pronounced pyramidal character of ReO₃ in the latter molecule. ^b Topological charge defined by integrating the density into the domains defined by the surfaces of zero gradient flux.²⁷

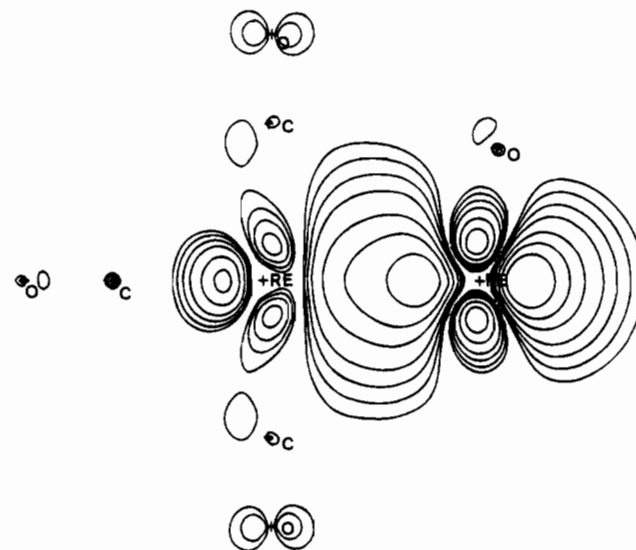


Figure 3. O₃Re–Re(CO)₅: plot of the electron density generated along the metal–metal axis by the active orbitals (σ and σ*) of the TCSCF calculation.

bonding density is not restricted to pure d_{z²} orbitals overlapping along the Re–Re axis: it extends up and down, reflecting the d_{z²}/6s hybrid character of the bonding orbital. It is clear from this plot, as from the table of orbital populations (Table 3) that the bonding presents the character of a σ donation from [ReO₃]⁻ toward [Re(CO)₅]⁺. According to the Mulliken population analysis, 72.5% of the bonding density should be attributed to the trioxorhenium fragment. The bonding orbital of **1** is quite similar to that of the AFW complex, as evidenced by the resemblance between the Mulliken metal populations of trioxorhenium in both complexes: 0.717 e in O₃Re–ReCl₂(H₂PCH₂PH₂)₂, and 0.735 e in **1**. The distribution of this population among the atomic orbitals is also comparable for both molecules (Table 3). The different magnitude of the electron transfers toward ReO₃ (0.785 e for the AFW complex, 0.534 e for **1**) therefore does not affect either the population of the metal atom

(27) (a) Bader, R. F. W. *Acc. Chem. Res.* **1975**, *8*, 34–40. (b) Bader, R. F. W. *Ibid.* **1985**, *18*, 9–15. (c) Bader, R. F. W.; Nguyen-Dang, T. *Adv. Quantum Chem.* **1981**, *14*, 63–124. (d) Bader, R. F. W. *Atoms in Molecules. A Quantum Theory*; Clarendon Press, Oxford, 1990.

Table 4. Critical Points of the Distribution of ρ and of $-\nabla^2\rho$ for $\text{O}_3\text{Re}-\text{Re}(\text{CO})_5$

atoms	ρ	$\nabla^2\rho$	distance (Å)	location
Saddle Point of ρ^a along the Re(VI)–Re(0) Bond Axis				
Re–Re	0.060	0.11	Re(0): 1.22 Re(VI): 1.57	
Maxima in $-\nabla^2\rho^b$				
Re(0)	1.044	-13.15	0.45	bisector $\pm x + y - z$ (*2)
Re(0)	1.042	-13.09	0.45	bisector $\pm x, -y - z$ (*2)
Re(0)	1.044	-13.03	0.45	bisector $\pm x + y + z$ (*2)
Re(0)	1.046	-13.07	0.45	bisector $\pm x - y + z$ (*2)
Re–Re	0.076	-0.006	Re(0): 1.5 Re(VI): 1.3	Re–Re axis (int.)
Re(VI)	0.988	-11.57	0.46	Re–Re axis (int)
Re(VI)	1.070	-13.85	0.45	Re–Re axis (ext)
Re(VI)	1.086	-14.63	0.45	Re–O (ext) (*3) ^c
C _{ax}	0.324	-1.08	0.47	C _{ax} –Re
C _{eq}	0.329	-1.14	0.46	C _{eq} –Re (*4)
Minima in $-\nabla^2\rho^d$				
Re(0)	0.302	2.09	0.74	Re–Re axis (int)
Re(0)	0.316	2.27	0.73	Re(0)–C _{ax}
Re(0)	0.307	2.27	0.73	Re(0)–C _{eq} (*4)

^a (3,–1) critical point. ^b (3,–3) critical points (charge concentration sites). ^c The pc–Re–O angle is 178.9° (see Figure 5a). ^d (3,+3) critical points (charge depletion sites).

in ReO_3 or the nature of the bonding. The amount of the electron transfer in $\text{O}_3\text{Re}-\text{L}$ molecules (Table 2) illustrates the destabilization of the SOMO in L, especially large for $\text{ReCl}_2(\text{dmpm})_2$. In 1, the decrease of the electron transfer only affects the basicity of the oxygen sphere surrounding the metal. The bond energy between the two metal fragments appears to be strongly correlated with the amount of charge transferred to ReO_3 , but the nature of the metal–metal coupling basically remains a σ donation from the most oxidized rhenium atom to the least oxidized one.

3.3. Laplacian Distribution of the Charge Density. The critical points of the Laplacian distribution of the charge density^{28–30} issued from the SCF wave function of $\text{O}_3\text{ReRe}(\text{CO})_5$ are reported in Table 4, and a plot of $\nabla^2\rho$ is displayed in the plane of symmetry containing two axial Re–CO bonds and one Re–O bond (Figure 4). The distribution of those critical points is quite different around Re(VI) and Re(0)³¹ and provides landmarks to point out the distinct nature of the metal–ligand bonding. Eight critical points of the type (3,–3), that is, local

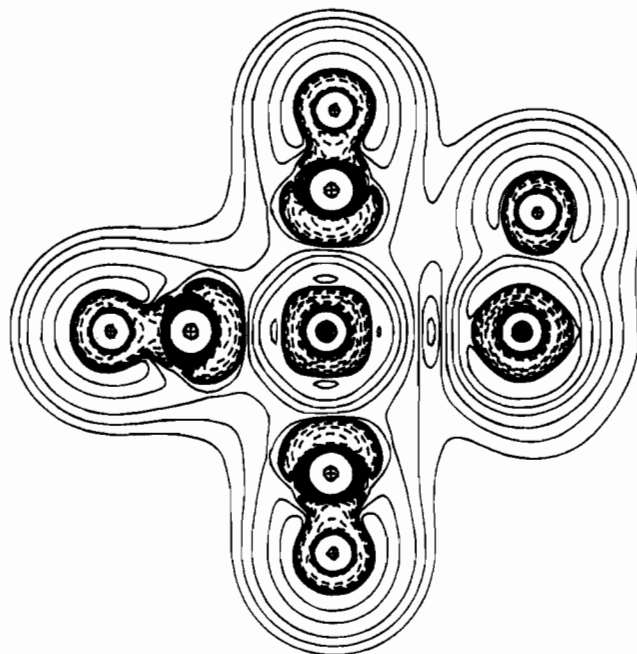


Figure 4. $\text{O}_3\text{Re}-\text{Re}(\text{CO})_5$: plot of $\nabla^2\rho$ in the molecular plane of symmetry, assuming a C_s conformation; solid lines are shown for $\nabla^2\rho > 0$ (regions of charge depletion) and dotted lines for $\nabla^2\rho < 0$ (regions of charge concentration).

maxima in $-\nabla^2\rho$, are surrounding Re(0) as the apices of a cube. Such a distribution is easily interpretable in the case of d^6 complexes in an octahedral environment. The eight (3,–3) critical points correspond to maxima of charge concentration located in the region of maximal overlap between the three occupied t_{2g} -like metal orbitals. A similar distribution of (3,–3) critical points around metal atoms has been already characterized in $\text{Mn}_2(\text{CO})_{10}$,³² but also in $\text{Fe}_2(\text{CO})_9$ ³² and in the nonsymmetric binuclear complex $\text{Rh}_2(\text{tcl})_4$, with $\text{tcl} = \text{NC}(\text{S})-(\text{CH}_2)_2(\text{CH}_2)$.³³

Five (3,–3) critical points are found in the vicinity of the metal in the trioxorhenium moiety. Three of those charge concentration regions, the highest ones in terms of $-\nabla^2\rho$, are oriented in the directions opposite to the Re–O bonds (Figure 5a). A similar orientation of the maxima in $-\nabla^2\rho$ has been obtained around the Mo(IV) metal atom in $\text{Mo}_2(\text{PH}_3)_4(\text{OCH}_3)_4$ (Figure 5b).³⁴ This distribution is also consistent with the (3,–3) critical points being characterized in the directions opposite to those of the strongest V–O bonds in $[\text{V}_{10}\text{O}_{28}]^{6-}$.³⁵ In this latter molecule, the maxima of charge concentration in the vicinity of the metal could be correlated with regions of local density accumulations (in terms of ρ) scattered around the globally depleted vanadium atoms.³⁵ Such local accumulations occurring in a depleted region in the direction opposite to the bond axis (or opposite to the axis of the strongest bond) have been associated with the cationic term of an ionic interaction.³⁶

The two last (3,–3) critical points characterized in the vicinity of Re(VI) both appear along the z axis, one away from and the second toward Re(0) (Figure 5a). It has been shown that the local concentrations of charge in the valence shell of an atom

- (28) (a) Bader, R. F. W.; Essén, H. *J. Chem. Phys.*, **1984**, *80*, 1943–1960. (b) Bader, R. F. W.; MacDougall, P. J.; Lau, C. D. H. *J. Am. Chem. Soc.* **1984**, *106*, 1594–1605.
- (29) (a) Bader, R. F. W.; Gillespie, R. J.; MacDougall, P. J. *J. Am. Chem. Soc.* **1988**, *110*, 7329–7336. (b) MacDougall, P. J.; Hall, M. B.; Bader, R. F. W.; Cheeseman, J. R. *Can. J. Chem.* **1989**, *67*, 1842–1846.
- (30) The guidelines and the technical terms used to discuss the Laplacian distribution of the electron density have been defined by R. F. W. Bader. Some of these definitions are reproduced here. The Laplacian of a scalar field as the electronic charge density determines where the field is locally concentrated, that is, where $\nabla^2\rho < 0$, and where it is locally depleted (where $\nabla^2\rho > 0$). Since electronic charge is concentrated where $\nabla^2\rho < 0$, it has been found to be convenient to focus the discussion on the function $-\nabla^2\rho$, since a maximum in this function corresponds to a maximum in charge concentration.^{27a} Each critical point in $\nabla^2\rho$ is classified by the number of nonzero eigenvalues (its rank) and the algebraic sum of the signs of the eigenvalues (its signature). A minimum in $-\nabla^2\rho$, a local depletion of charge, exhibits three positive eigenvalues and is referred to as a (3,+3) saddle point. A maximum in $\nabla^2\rho$ is a (3,–3) critical point, and saddle points may be either (3,+1) or (3,–1) critical points.^{28b}
- (31) The formal oxidation states associated throughout the text with the rhenium atoms in $\text{O}_3\text{Re}-\text{Re}(\text{CO})_5$ have been assigned assuming the ReO_3 and $\text{Re}(\text{CO})_5$ moieties to be neutral. It is clear that assigning respective oxidation states of V and I to rhenium in ReO_3 and $\text{Re}(\text{CO})_5$ would be more consistent with the intramolecular charge transfer evidenced from the calculations.

- (32) Bo, C.; Sarasa, J.-P.; Poblet, J.-M. *J. Phys. Chem.* **1993**, *97*, 6362–6366.
- (33) Bo, C.; Poblet, J. M.; Bénard, M. *Chem. Phys. Lett.* **1990**, *169*, 89–96.
- (34) Bo, C. Ph.D. Thesis, Tarragona, 1992, 135–140.
- (35) Kempf, J.-Y.; Rohmer, M.-M.; Poblet, J. M.; Bo, C.; Bénard, M. *J. Am. Chem. Soc.* **1992**, *114*, 1136–1146.
- (36) Bader, R. F. W.; Henneker, W. H. *J. Am. Chem. Soc.* **1965**, *87*, 3063–3068.

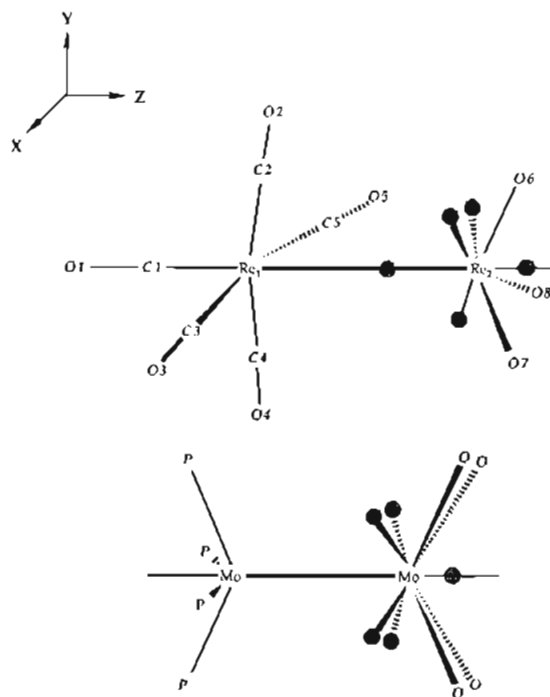
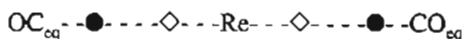
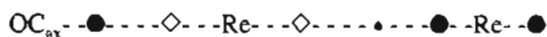


Figure 5. Spatial distribution of the maxima in $-\nabla^2\rho$ in the valence shell of charge concentration (VSCC) (a) of Re(VI) in $\text{O}_3\text{Re}-\text{Re}(\text{CO})_5$ and (b) of Mo(IV) in $\text{Mo}_2(\text{Ph}_3\text{P})_4(\text{OCH}_3)_4$.

in a molecule can be assimilated with the spatially localized electron pairs of the VSEPR model.²⁹ The charge concentrations characterized along the z axis in the vicinity of Re(VI) should be associated with the filled d_{z^2} orbital of this atom and highlight the donor character of the negatively charged trioxorhenium moiety. No such maximum in $-\nabla^2\rho$ was found around the z axis in the vicinity of Re(0). Facing the trioxorhenium fragment, Re(0) behaves as an acceptor, as deduced from the population analysis. This behavior, characterized by a weakly populated d_{z^2} orbital (0.499 e, Table 3), is materialized in the Laplacian distribution by means of a local *minimum* in $-\nabla^2\rho$, a (3,+3) critical point along the z axis directed toward Re(VI). Four other, more prominent (3,+3) critical points are characterized, as expected, in the direction of the CO ligands (Table 4). The lone pair of each carbon monoxide ligand pointing toward the metal generates a charge concentration site, that is, a (3,-3) critical point. This maximum in $-\nabla^2\rho$ faces the minimum located on the metal side:



Let us be reminded that a similar arrangement, typical of donor-acceptor interactions, has been characterized along the metal-metal axis, with a (3,+3) point in the vicinity of Re(0) and a (3,-3) point close to Re(VI). A third critical point of the (3,-3) type has been characterized, however, along the Re-Re line, at 1.3 Å from Re(VI). The value of $\nabla^2\rho$ is -0.006 au at this point (Table 5), corresponding to a very small region of charge concentration in a depleted environment:



A similar concentration ($\nabla^2\rho = -0.01$ au, $\rho = 0.03$ e/au³) had been characterized at the center of the Mn-Mn bond in $\text{Mn}_2(\text{CO})_{10}$.³² In this symmetric complex, the (3,-3) critical point is coincident with the saddle point [(3,-1) critical point] in the charge density distribution, ρ , which corresponds to the signature of the Mn-Mn bond.³⁷ A saddle point in ρ is also found along the Re(0)-Re(VI) axis of **1** ($\rho = 0.06$ e/au³, $\nabla^2\rho = 0.11$ au,

Table 5. Bonding Energetics for $\text{O}_3\text{Re}-\text{Re}(\text{CO})_5$: Ab Initio Closed-Shell SCF (Referred to as CS) or Open-Shell SCF (Referred to as OS), TCSCF, and Configuration Interaction (CI)^a Energies Obtained for (1) $\text{O}_3\text{Re}-\text{Re}(\text{CO})_5$, (2) ReO_3 , and (3) $\text{Re}(\text{CO})_5$

molecule	level of comput	geometry	sym	state	energy (hartrees)
1	SCF(CS)	optim ^b	C_s	$^1A'$	-944.114 479
	TCSCF	optim ^b	C_s	$^1A'$	-944.128 638
	CI ₂	optim ^b	C_s	$^1A'$	-944.132 701
(2)⁻	SCF(CS)	unrel ^c	C_{3v}	1A_1	-302.828 190
	TCSCF	unrel ^c	C_{3v}	1A_1	-302.836 307
	CI ₂	unrel ^c	C_{3v}	1A_1	-302.842 195
	SCF(CS)	optim ^d	D_{3h}	$^1A'_1$	-302.836 085
	TCSCF	optim ^d	D_{3h}	$^1A'_1$	-302.841 233
(3)⁺	SCF(CS)	unrel ^c	C_{4v}	1A_1	-641.077 236
	SCF(CS)	optim ^e	C_{4v}	1A_1	-641.077 752
	(2) ⁻ + (3) ⁺	corr ^f	optim ^{d,e}		-943.926 492
Re-Re bond energy					0.206 209
2	SCF(OS)	unrel ^c	C_{3v}	2A_1	-302.702 441
	SCF(OS)	optim ^d	D_{3h}	$^2A'_1$	-302.704 483
	SCF(OS)	unrel ^c	C_{4v}	2A_1	-641.321 724
3	SCF(OS)	optim ^e	C_{4v}	2A_1	-641.325 062
	SCF(OS)	optim ^{d,e}			-944.029 545
2 + 3					0.103 156
Re-Re bond energy (SCF)					
1	CI ₂₆	optim ^b	C_s	$^1A'$	-944.588 163
2 + 3	CI ₂₆	optim ^{d,e}	C_s	$^3A'$	-944.487 068
Re-Re bond energy (CI ₂₆)					0.101 095

^a CI₂ = 2 correlated electrons, belonging to the $\sigma_{\text{Re-Re}}$ bonding orbital; CI₂₆ = 26 correlated electrons; see section 2.2. ^b Optimization of the molecular geometry at the SCF level: Re-Re = 2.789 Å, Re-O = 1.698 Å, Re-Re-O = 97.5°, Re-Re-C = 88.0°. ^c Same geometry as in the molecule. ^d See Table 2 in ref 1a. ^e Optimization of the pyramidalization angle: Re-Re-C = 88.9° for (3)⁺; 84.6° for **3**. ^f Pair correlation included.

table 4). This (3,-1) critical point in the distribution of ρ is shifted by 0.27 Å toward Re(0) with respect to the minimum in $\nabla^2\rho$. It is noteworthy that the topology of the Laplacian of charge density along the Re-Re bond simultaneously displays the characters of a donation interaction [the (3,+3) and the (3,-3) critical points in the vicinity of the metal atoms] and those of a covalent bond [the (3,-3) critical point in the central part of the bond]. The characterization of those critical points substantiates the analysis of the bonding made above from fragment orbital interactions and atomic orbital populations.

4. Bonding Energetics

The energies computed at the SCF, TCSCF, and CI levels for **1** and for the fragments ReO_3 and $\text{Re}(\text{CO})_5$ either unrelaxed or in their optimized geometry are reported in Table 5. Dissociation into ionic fragments [ReO_3]⁻ and [$\text{Re}(\text{CO})_5$]⁺ has also been considered. Table 6 displays similar information concerning $\text{O}_3\text{Tc}-\text{Tc}(\text{CO})_5$. The main results are illustrated in Figure 6 for $\text{O}_3\text{Re}-\text{Re}(\text{CO})_5$ and in Figure 7 for the complex of technetium. The results previously obtained for $\text{O}_3\text{Re}-\text{Re}(\text{H}_2\text{PCH}_2\text{PH}_2)_2$ are reproduced in Figure 8.

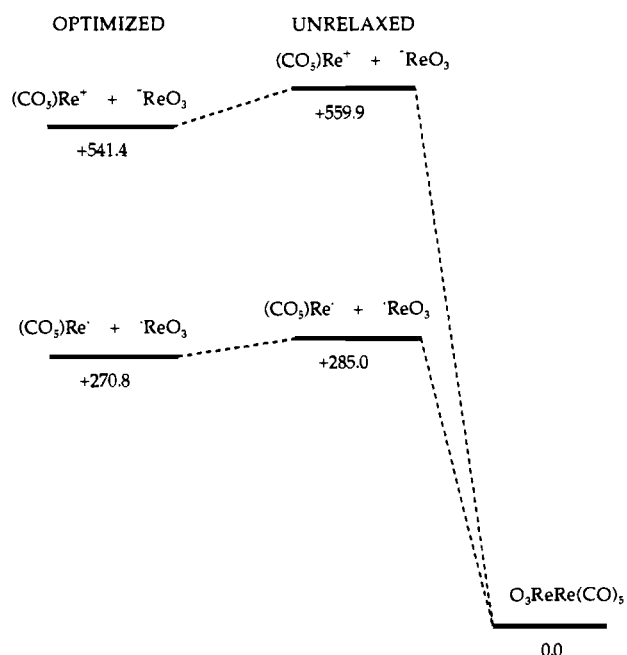
Trioxorhenium has been presented as a powerful electron attractor.³⁰ As a matter of fact, its electron affinity is computed to be 3.36 eV (Tables 1 and 5). The value is quite similar for trioxotechnetium (Table 6). In $\text{O}_3\text{Re}-\text{ReCl}_2(\text{H}_2\text{PCH}_2\text{PH}_2)_2$, this electron affinity was almost sufficient to counterbalance the low ionization energy of the Re(II) fragment shaped as a pentagonal pyramid: the dissociation into unrelaxed ionic fragments was no more than marginally disadvantaged with respect to homolytic cleavage (Figure 8).

(37) Low, A. A.; Kunze, K. L.; MacDougall, P. J.; Hall, M. B. *Inorg. Chem.* **1991**, *30*, 1079-1086.

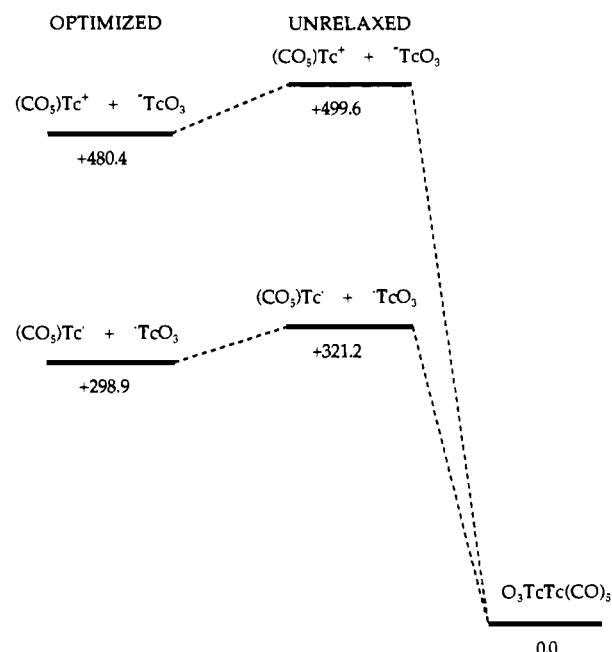
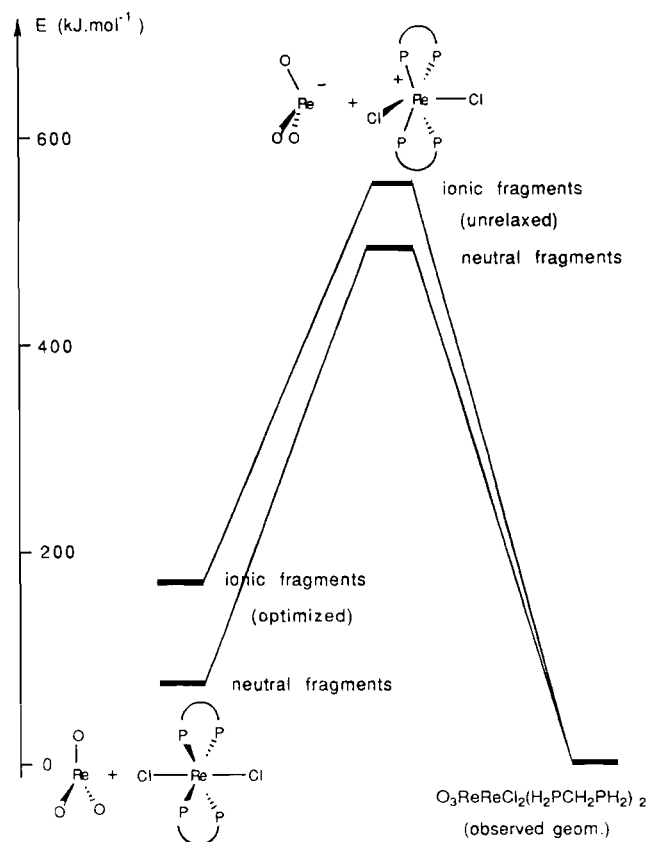
Table 6. Bonding Energetics for $O_3Tc-Tc(CO)_5$: Ab Initio Closed-Shell SCF (Referred to as CS) or Open-Shell SCF(OS), TCSCF, and CI Energies Obtained for (1) $O_3Tc-Tc(CO)_5$, (2) TcO_3 , and (3) $Tc(CO)_5$

molecule	level of comput	geometry	sym	state	energy (hartrees)
1	SCF(CS)	optim ^a	C_s	$^1A'$	-9179.617 72
	TCSCF	optim ^a	C_s	$^1A'$	-9179.664 36
	CI	optim ^a	C_s	$^1A'$	-9179.667 71
(2) ⁻	SCF(CS)	unrel ^b	C_{3v}	1A_1	-4420.411 24
	TCSCF	unrel ^b	C_{3v}	1A_1	-4420.417 02
	CI	unrel ^b	C_{3v}	1A_1	-4420.420 90
	SCF(CS)	optim	D_{3h}	$^1A'_1$	-4420.411 67
(3) ⁺	TCSCF	optim	D_{3h}	$^1A'_1$	-4420.417 37
	CI	optim	D_{3h}	$^1A'_1$	-4420.421 50
	SCF(CS)	unrel ^b	C_{4v}	1A_1	-4759.056 51
	SCF(CS)	optim	C_{4v}	1A_1	-4759.063 26
(2) ⁻ + (3) ⁺	correl ^c	optim			-9179.484 76
Tc-Tc bond energy					0.182 95
2	SCF(OS)	unrel ^b	C_{3v}	2A_1	-4420.274 01
	SCF(OS)	optim	D_{3h}	$^2A'_1$	-4420.277 12
3	SCF(OS)	unrel ^b	C_{4v}	2A_1	-4759.271 37
	SCF(OS)	optim	C_{4v}	2A_1	-4759.276 75
2 + 3		optim			-9179.553 87
Tc-Tc bond energy					0.113 84

^a Complete optimization of the molecular geometry with TURBO-MOLE (see Figure 2). ^b Same geometry as in the molecule. ^c Pair correlation included.

**Figure 6.** Bonding energetics of $O_3Re-Re(CO)_5$. Relative energy (kJ mol^{-1}) of the isolated fragments, either ionic or neutral in their optimal geometry (left-hand side), and in their unrelaxed conformation (center) with respect to the complex in its optimized geometry (right-hand side).

The ionization of $Re(CO)_5$ leading to a cation with a closed-shell structure requires 6.73 eV , that is 650 kJ mol^{-1} . Even though this energy is in the expected range for the ionization of a metal d electron, it is sufficiently large to rule out an ionic path to dissociation. The homolytic cleavage into neutral, open-shell fragments is computed to require 285 kJ mol^{-1} when the isolated fragments retain the geometry that has been optimized in the binuclear complex. This bond energy between the two rhenium fragments is little more than half the bond energy computed between the neutral, unrelaxed fragments of $O_3Re-ReCl_2(H_2PCH_2PH_2)_2$ (500 kJ mol^{-1}). This decrease of the bond energy should be interpreted in terms of a less energetically favorable charge transfer. At variance from the AFW complex,

**Figure 7.** Bonding energetics of $O_3Tc-Tc(CO)_5$. See caption for Figure 6.**Figure 8.** Bonding energetics of $O_3Re-ReCl_2(H_2PCH_2PH_2)_2$ (from ref 1a). See caption for Figure 6.

however, the geometrical relaxation of the isolated fragments remains of little importance. Pyramidalization of ReO_3 and slight angular changes in $Re(CO)_5$ lead to an energy difference of 14 kJ mol^{-1} with respect to optimized fragments.³⁸ Remember that the $Re-CO$ distances were retrieved from $Re_2(CO)_{10}$ ²⁴ and were not subject to optimization. At variance from that, a complete geometry optimization was carried out on both $O_3Tc-Tc(CO)_5$ and the isolated technetium fragments, leading to a relaxation energy (22 kJ mol^{-1}) that is not significantly

different (Figure 7). A comparison with the AFW complex speaks for itself: a large part of the sizeable attractive potential between the rhenium fragments was used to activate those fragments into conformations favorable to charge transfer and to complexation.^{1a} The net bond energy with respect to *relaxed* fragments was eventually 78 kJ mol⁻¹ (Figure 8). In complex **1**, the attractive potential between the two rhenium fragments is by far lower, but the reorganization required for the fragments is minimal, and the bond energy amounts to 271 kJ mol⁻¹ (299 kJ mol⁻¹ for O₃Tc–Tc(CO)₅). This bond energy is higher than the values computed at the same level of approximation for a series of O₃Re–L complexes (Table 2). This represents an encouraging information concerning the design of new routes toward the synthesis of binuclear complexes undergoing intramolecular disproportionation.

5. Summary and Conclusion

An obvious application of the isolobal analogy shows that the hypothetical binuclear complex O₃Re–Re(CO)₅ is expected to display an electronic structure similar to that of various known complexes of the type O₃Re–L (L = CH₃, C₂H₅, CH₂Si(CH₃)₃, C₆(CH₃)_nH_{5–n}, Cl, F).^{8–11} Ab initio CI calculations show that O₃Re–Re(CO)₅ and its technetium analog would be characterized by an important charge transfer toward the MO₃ fragment. Because of this charge transfer, the bonding between trioxorhenium and Re(CO)₅ presents important analogies with that described for the unique bimetallic complex of ReO₃ characterized to date, O₃Re–ReCl₂(dmpm)₂. The amount of the electron transfer in O₃Re–Re(CO)₅ is however less massive than for this latter complex due to the less destabilized character of the

SOMO in the Re(CO)₅ fragment. The metal–metal distance computed for O₃Re–Re(CO)₅ is intermediate between the long bond length (3.04 Å) observed for Re₂(CO)₁₀ and the very short one (2.4705 Å) characterized for O₃Re–ReCl₂(dmpm)₂. As for the latter complex, the Re–Re bond in O₃Re–Re(CO)₅ presents the character of a σ donation from the most oxidized metal atom to the least oxidized one. Bader's topological analysis of the Laplacian distribution of the density leads to the characterization of three critical points along the metal–metal bond axis. The minimum in $-\nabla^2\rho$ close to Re(0), and the maximum located in the vicinity of Re(VI) are altogether characteristic of a donation interaction from ReO₃ to Re(CO)₅. The (3,–3) maximum in $-\nabla^2\rho$ evidencing the existence of a small region of shallow charge concentration in the central part of the bond axis should be rather interpreted as an indication for covalent bonding. The energy required for a homolytic dissociation into neutral, unrelaxed fragments is computed to be 285 kJ mol⁻¹. The bond energy computed for O₃Re–ReCl₂(H₂PCH₂PH₂)₂ was computed to be twice as much, but most of this energy was used to activate the ReCl₂(dmpm)₂ fragment into a pentagonal pyramid conformation. In O₃Re–Re(CO)₅, the relaxation energy of the fragments is minimal, and the energetic balance with respect to fragments with relaxed geometry (–271 kJ mol⁻¹) appears extremely favorable when compared to the case of various O₃Re–L complexes.

Acknowledgment. We are very much indebted to Prof. W. A. Herrmann for providing incentive to the present work. Calculations have been carried out in part on an IBM RS 6000 workstation purchased with funds provided by DGICYT of the Government of Spain (PB89-0648-C02-02), in part of the Cray-YMP of the Centre de Supercomputacio de Catalunya (Barcelona, Spain), and in part on the Cray computers of the Centre de Calcul Vectoriel de la Recherche (Palaiseau, France) and of the CNRS (IDRIS, Orsay, France). We are pleased to thank Prof. R. F. W. Bader for a copy of the AIMPAC package of programs, and Dr. Carles Bo for fruitful discussions.

(38) The bond energy with respect to optimized fragments (0.103 156 hartrees, that is, 271 kJ mol⁻¹) has been obtained at the TCSCF + CI level of calculation for the bimetallic complex. Only the two d metal electrons involved in the σ bond have been correlated (Table 5). At a more extended level of correlation (26 outer valence electrons correlated, see section 2.2) the bond energy was found to change very little (0.101 095 hartrees, that is, 265 kJ mol⁻¹).